# CHIRAL TETRATHIAFULVALENE PRECURSORS FOR CRYSTALLINE MOLECULAR CONDUCTORS

- PhD Thesis Summary -

**Alexandra BOGDAN**

**Review Committee:**

| | | |
|---|---|---|
| President: | Prof. Dr. Cristian Silvestru | Professor, Babeș-Bolyai University, Romania |
| Reviewers: | Dr. Stéphane Bellemin-Laponnaz | Research Director, Université de Strasbourg, France |
| | Prof. Dr. Petre Ioniță | Professor, Bucharest University, Romania |
| | Dr. Anamaria Terec | Associate Professor, Babeș-Bolyai University, Romania |
| | Dr. Nicolas Vanthuyne | Research Engineer, Aix Marseille Université, France |

**Scientific Advisors**:

| | |
|---|---|
| **Prof. Dr. Ion Grosu** | **Professor, Babeș-Bolyai University, Romania** |
| **Dr. Narcis Avarvari** | **Research Director, Université d'Angers, France** |
| **Dr. Flavia Pop** | **Scientific Researcher, Université d'Angers, France** |

***Cluj-Napoca***
***2022***

# Table of contents

# Table of Contents of the Summary

# General introduction

Over the last decades it was demonstrated that the chirality is an important tool when it comes to the formation of conducting materials, as it highly impacts the packing pattern, therefore, the conducting properties. Thus, this study is devoted to the development of new chiral TTF derivatives as precursors for the synthesis of novel conducting materials.

The first chapter covers an introduction to the TTF based conducting molecular materials along with the importance of chirality in electroactive systems, as well as a short description of the synthetic methods used for the formation of these type of materials.

The second chapter introduces the spiranes in TTF chemistry, as axial chirality inducers. So far, spiro derivatives have been very little investigated as building blocks for TTF based conducting precursors. Spiro-TTFs with one and three chiral centres have been synthesized following a direct approach *via* the Diels-Alder reaction or a multi-step synthetic strategy. The chiroptical investigation of these systems revealed a significant difference in chiroptical activity not only between the one and three chiral centres versions, but also between diastereomers of the latter. Charge transfer complexes of the one chiral centre spiro-TTF with $TCNQF_2$ and $TCNQF_4$ are also reported.

The third chapter focuses on the point chirality in TTF derivatives. A new chiral heterocycle-fused TTF precursor has been synthesized, together with its family of TTF derivatives. Charge transfer complexes with $TCNQF_4$ and radical cation salts with various anions of the new donors are reported, and their structure is discussed.

The fourth chapter discusses the radical cation salts of two of the representative chiral TTFs (TM-BEDT-TTF and Me-EDT-TTF) with three anions, including iridium magnetic anions. A new TTF conductor with potential magnetic properties is reported.

Finally, the last chapter consists in the synthesis and characterization of some novel miscellaneous TTF derivatives, designed as suitable precursors for electroactive materials.

# List of chiral precursors and donors

## Chapter 2 – new chiral precursors and donors

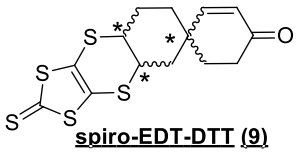

spiro-EDT-DTT (9)

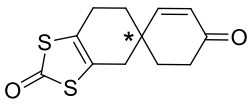

spiro-DTO (15)

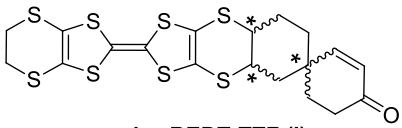

spiro-BEDT-TTF (I)

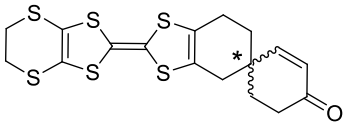

spiro-EDT-TTF (II)

## Chapter 3 – new chiral precursor and donors

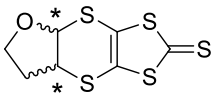

THF-EDT-DTT (16)

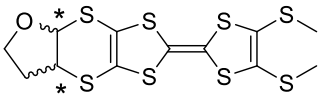

THF-EDT-TTF-bis(SMe) (III)

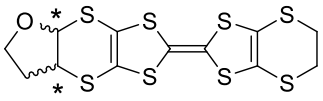

THF-BEDT-TTF (IV)

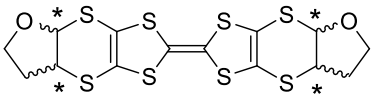

BTHF-BEDT-TTF (VI)

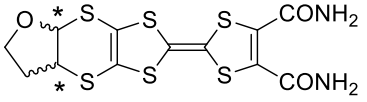

THF-EDT-TTF-bis($CONH_2$) (VIII)

## Chapter 4

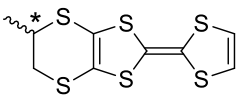

Me-EDT-TTF

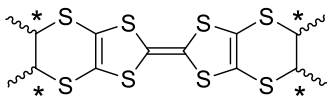

TM-BEDT-TTF

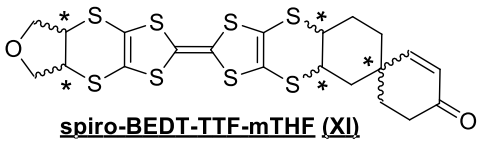

spiro-BEDT-TTF-mTHF (XI)

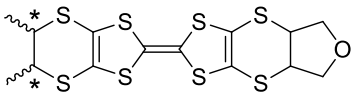

DM-BEDT-TTF-mTHF (XII)

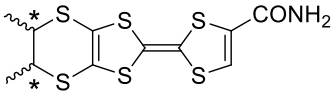

DM-EDT-TTF-$CONH_2$ (XIII)

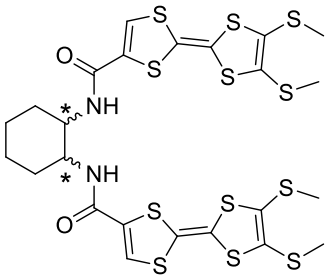

cyclohexane-diamide-bis(TTF) (XIV)

# Chapter 1

# Tetrathiafulvalene (TTF) molecular conductors and chirality

# *1.1 Scientific background*

Multifunctional materials are the subject of a tremendous research effort among the scientists around the world. The concept of combining multiple properties within the same compound, which can coexist or interplay, led to a relatively recent challenge, namely investigation of the impact on the physical properties of a molecular conductor by introducing a chiral motif in its structure.

Tetrathiafulvalene (TTF) and its derivatives are ones of the most significant electroactive precursors [1] for organic conductors and superconductors [2] due to its strong electron-donor ability and the advantage of having reversible redox properties (***Figure 1.1***).

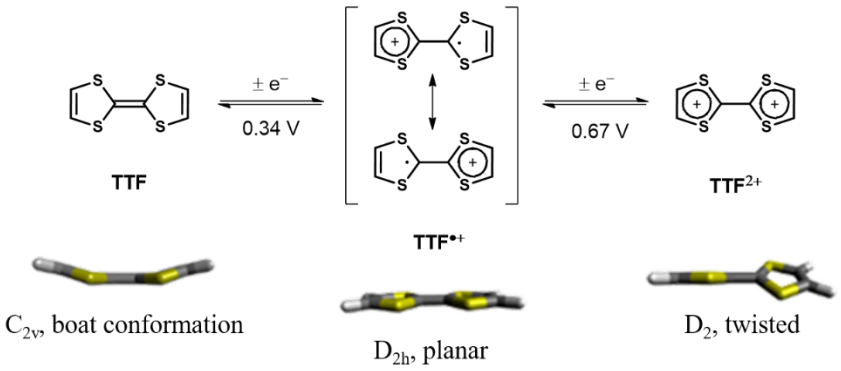


***Figure 1.1***. Neutral, radical cation and dication forms of TTF

Some of the benefits of associating chirality to electroactivity consist in the control of supramolecular chirality in electroactive helical aggregates, the possibility to tune the chiroptical properties, or the modulation of the structural disorder in solid state. Moreover, in the case of chiral TTFs, different packing patterns and crystalline space groups observed in mixed valence salts led to a continuous development of the synthesis and use of chiral TTF derivatives in chiral molecular conductors [3]. In this particular case differences in conductance have been observed in mixed valence salts of chiral TTFs such as: ethylenedithio-TTF-oxazolines (EDT-TTF-Ox) where the enantiomeric forms show superior conductance than the racemic one due to structural disorder effects [4], DM-EDT-TTFs have proven metallic conductivity or semiconducting behaviour due to induction of different packing in the solid state which is modulated by the anion size [5] and have been recently used to detect the electrical magneto-chiral anisotropy (eMChA) effect in bulk crystalline enantiopure conductors [6] , whereas TTF-helicene [7] , TTF-allene [8] and TTF-binaphthyl derivatives [9] have shown redox modulation of their chiroptical properties (***Figure 1.2***).

The peculiarity of these mixed valence salts, such as enantiomorphic space groups, packing of the molecules and conducting properties, certifies them as unprecedented examples where the asymmetry of the structure, namely chirality, has been found to have a direct influence on the electron transport and supramolecular structure of the material.

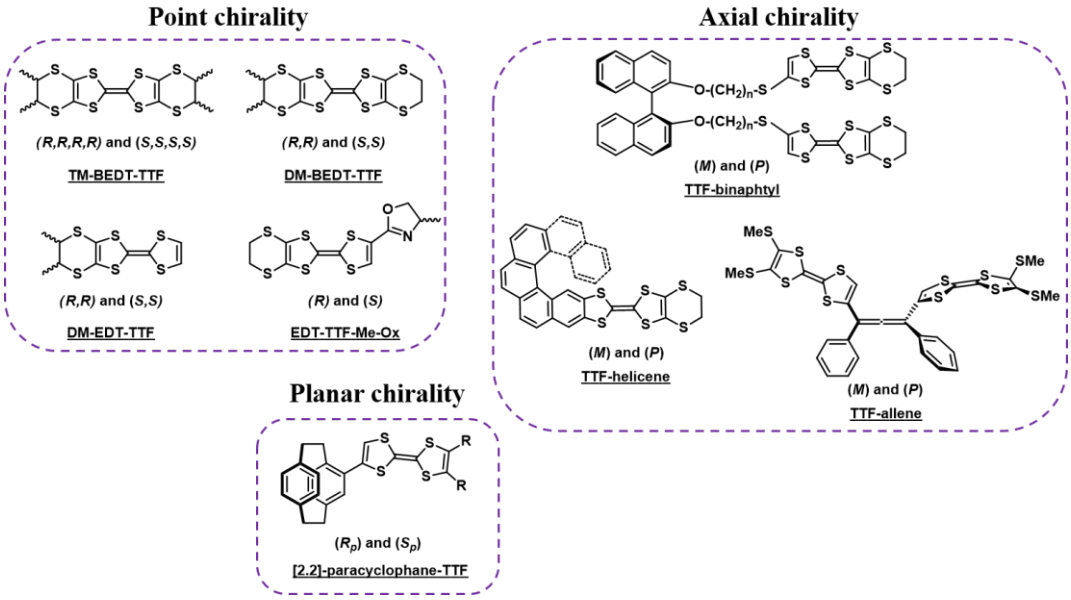


***Figure 1.2.*** Representative chiral TTF derivatives for each chirality type

# Chapter 2

# Spiro-TTFs for chiral electroactive materials

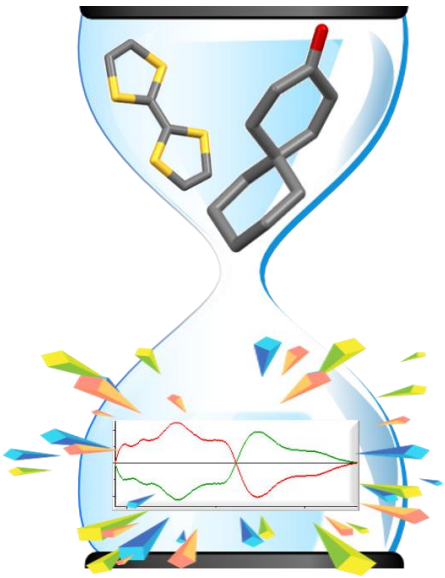

## 2.1 Literature data

The continuous development of the tetrathiafulvalene (TTF) based molecular conducting materials over the past decades includes a wide range of organic motifs used as building blocks for the functionalization of the TTF units. In order to increase the dimensionality of the organic conductors or to attain atypical optoelectronic properties, spirane units seem to be promising candidates for the design of new organic materials but at present they are little explored.

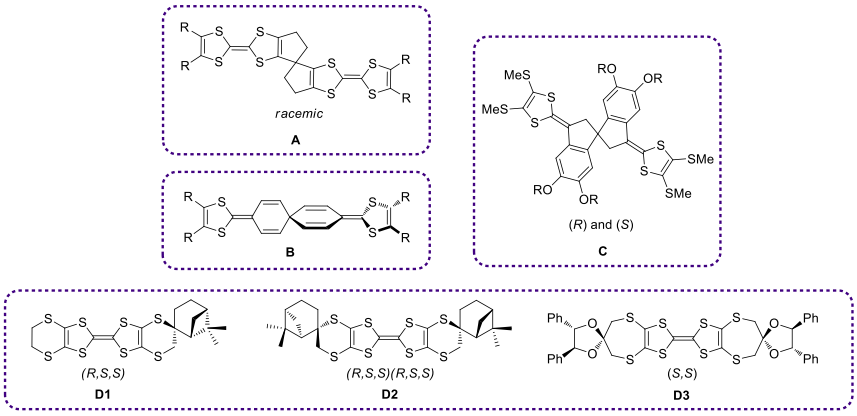


***Chart 2.1.*** TTFs containing spiro-framework described in the literature

The few literature data on spiro type derivatives decorated with TTF for molecular materials (***Chart 2.1***) [10,11,12,13] reveal some drawbacks such as multi-step synthesis and electrochemical instability but their potential for materials with increased dimensionality is yet to be revealed. In this context, one of the aims of this thesis work was to design and synthesize chiral spiro based TTF, using straightforward synthesis when possible, to characterize their electrochemical properties and to separate the enantiomers with the ultimate goal to use them in chiral molecular materials.

## 2.2 Results

This chapter is constructed around one of the main goals of the thesis project, which is the development of new molecular materials based on chiral spiro-TTF derivatives, where the impact of the spiro motif and its chirality on the arrangement of the molecules in the lattice could possibly lead to particular packings and interesting conducting properties.

## 2.2.1 Spiro-TTFs with three chiral centres

The spiro core **8**, reported by Martin et al [12] (***Scheme 2.1***), was used in this work as a dienophile in a Diels-Alder (D-A) pericyclic reaction with 1,3-dithiolane-2,4,5-trithione **T3** in order to obtain the bis(DT-DTT)spiro intermediate **9'** (***Scheme 2.1***). For our study, the benefit of this spiro unit lies in the presence of multiple functional groups that can undergo functionalization to afford various TTF derivatives. The **9'** compound was not observed in the reaction mixture, instead, two diastereomers **9A** and **9B** have been obtained.

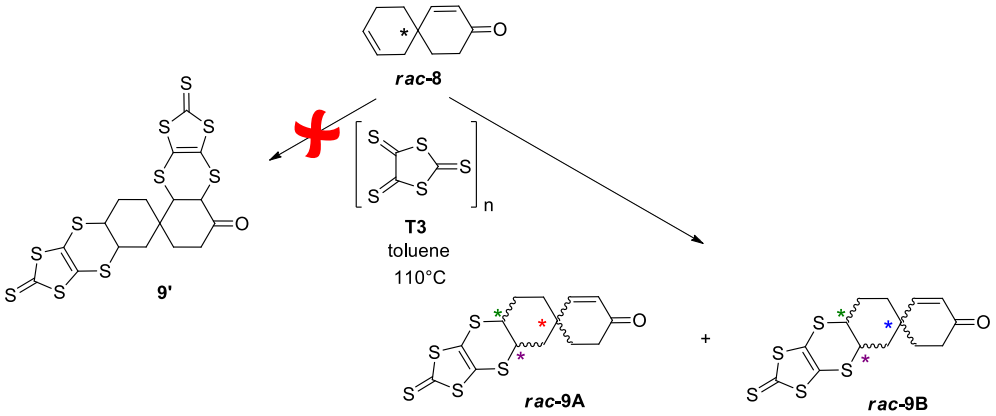


***Scheme 2.1.*** Synthesis of racemic mixtures **9A** and **9B** (*R,S,M* and *S,R,P*; *S,R,M* and *R,S,P*)

Because of the stereospecificity of the Diels-Alder reaction, the conjugated diene approaches the double bond on the spiro core in the *cis* position, entailing the resulting structure with a blocked *R,S* and *S,R* configuration of the two newly formed stereogenic centres. Due to this stereospecificity the $2^n$ (where n = number of the stereogenic centres) probability rule is not fulfilled, the *R,R* and *S,S* configurations of the two newly formed chiral carbon atoms not being obtained. Thus, only four stereoisomers resulted from the reaction. The diastereoisomers were partially isolated by conventional chromatography as two pairs of enantiomers (***rac*-9A** and ***rac*-9B**) with slightly different properties, as confirmed after structural analysis.

Suitable crystals for X-ray diffraction measurements were obtained by slow evaporation of the mixture of solvents (EtOEt/$CH_2Cl_2$ = 3/2 in the case of **9B** racemic form, and EtOEt/$CH_2Cl_2$ = 4/0.1 in the case of **9A** pair of enantiomers), at room temperature. A different crystal colour could be observed for the two racemic forms, namely yellow for the ***rac*-9A** and orange for the ***rac*-9B** (***Figure 2.1***), emphasizing the different packing of the two forms. The determined structures clearly show the different conformational arrangement of the dithiolene unit in the two pairs of stereoisomers (***Figure 2.1.***).

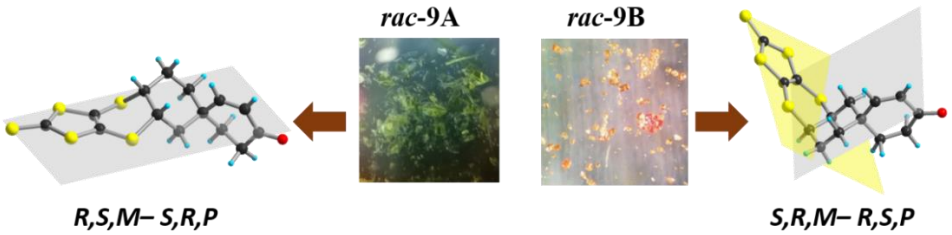


***Figure 2.1.*** Aspect of the two racemic forms of compound **9** in solid state (middle), and their determined structures (left and right side)

The absolute configuration of both systems was determined based on the single crystal structures. The *R,S,M-S,R,P* pair of enantiomers corresponds to the **9A** racemic mixture, while the *S,R,M-R,S,P* stereodescriptors are characterizing the **9B** stereoisomers. The *R,S* stereodescriptors were noted starting with the chiral carbon atom on the short edge of the spiro core (***Figure 2.2*** - red edge), while for the chirality of spiro motif, the stereodescriptors *M,P* were used, for a simplified general picture of the three chiral centres description.

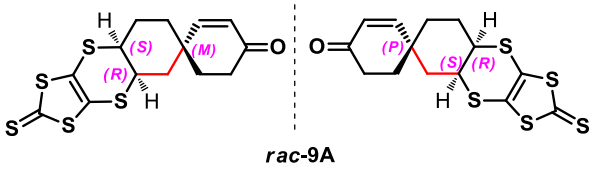


***Figure 2.2.*** Stereodescriptors assignment method for the three stereogenic centres

A mixture of the four stereoisomers was subjected to chiral separation using the chiral HPLC technique. The investigation of the chiroptical properties, using ECD spectroscopy and optical rotation measurements revealed further differences between the two sets of enantiomers. Thus, the two pairs of diastereomers exhibit different chiroptical properties, with a remarkable difference of ~ 200 degrees in optical rotations and different pattern of the CD waves. Furthermore, X-Ray diffraction measurements, corroborated with TD-DFT calculations, afforded the correct absolute configuration assignment and revealed that the type of the Cotton effect is not induced by the spiro chirality but by the two *R,S* and *S,R* stereogenic centres.

The two racemic forms, **9A** and **9B** respectively, were further engaged in a trimethyl phosphite mediated cross coupling reaction, at 150 °C for ~10 minutes, in order to obtain the target spiro-TTFs **I** (***Scheme 2.2***). The formation of the desired compounds was confirmed by mass spectrometry, NMR spectroscopy, as well by X-Ray diffraction measurements.

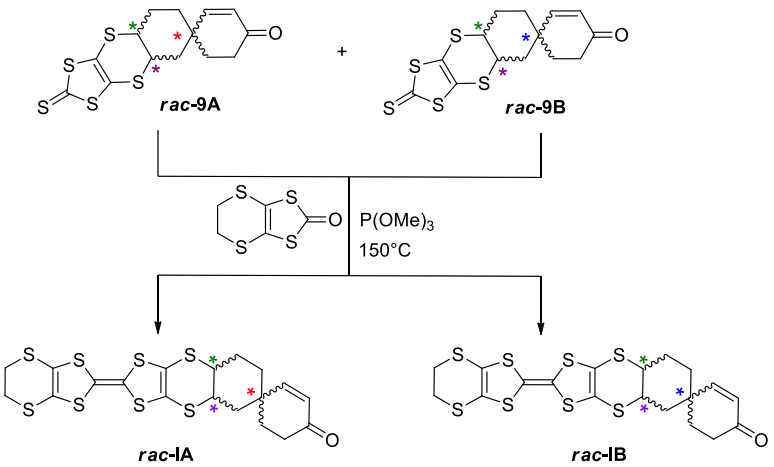


***Scheme 2.2.*** Synthesis of the spiro-TTFs ***rac*-IA** and ***rac*-IB**

The chiral separation of spiro-TTFs **I** was successfully performed through chiral HPLC and their chiroptical properties were investigated using the ECD spectroscopy and optical rotations measurements. The same difference of ~ 200 degrees in optical rotations and different pattern of the CD waves were maintained between the two sets of diastereoisomers but with an optical activity of approx. 200 degrees lower compared to the spiro derivatives **9**. Similar to the case of spiro derivatives 9, the absolute configuration assignment was based on both X-Ray diffraction measurements and TD-DFT calculations.

## 2.2.2 Spiro-TTFs with one chiral centre

Investigation of the spiro chirality behaviour was exclusively pursued as the next step for this study. In this respect, already reported synthetic procedures on related substrates were optimized on our spiro derivative **8**. The four steps synthetic strategy (***Scheme 2.3***) afforded the access to racemic **15** which was successfully obtained in 61% overall yield. All attempts to perform the addition on both double bonds have failed, probably due to lower reactivity induced by the neighbouring carbonyl unit. The formation of ***rac*-15** was confirmed by NMR spectroscopy and MS spectrometry, as well as by X-Ray diffraction measurements.

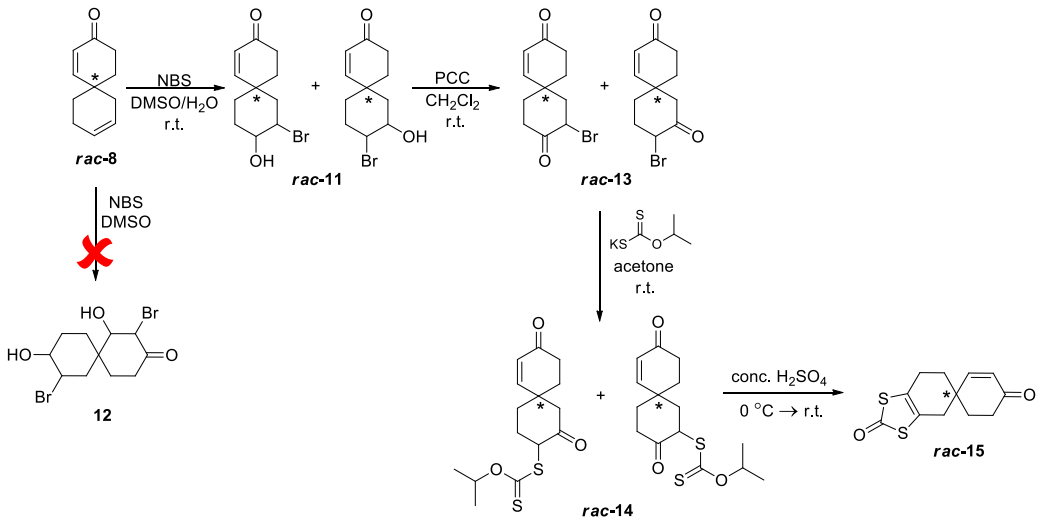


**Scheme 2.3.** Synthetic strategy for racemic compound **15**

Spiro derivative **15** was subjected to chiral separation through chiral HPLC. The chiroptical properties investigation, using ECD spectroscopy and optical rotations measurements revealed a low chiroptical activity as compared to the three chiral centre version **9**. Suitable crystals for X-ray diffraction measurements were obtained by slow evaporation of a solution of the second eluted enantiomer in acetonitrile. The enantiopure compound crystallized in the non-centrosymmetric monoclinic $P2_1$ space group, with two independent molecules in the asymmetric unit cell revealing further information on the packing behaviour of compound **15** (***Figure 2.3*** - bottom). The determined structure contains the *P* enantiomer as two conformers. The conformational difference between the two *P* molecules is based on the position of the carbon atom involved in the double bond, on the spiro carbon atom (***Figure 2.3*** – magenta bonds and atoms). Thus, the two conformers are labelled as *axial* and *equatorial*, respectively. The crystal structure of the *rac*-**15** compound shows the presence of only one of the two conformers, that is the *equatorial* one (***Figure 2.3*** - top).

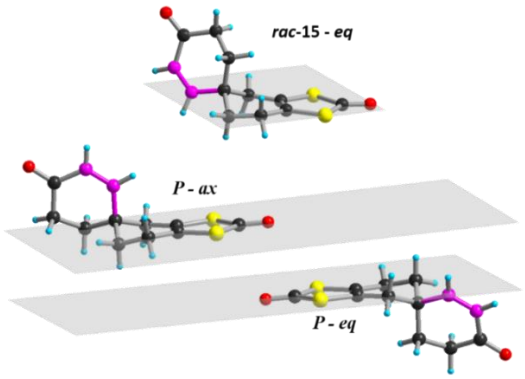


***Figure 2.3.*** Crystal structure of *racemic* (top) and *P* forms of compound **15** with emphasis on the conformational arrangement (magenta bonds and atoms)

The presence of the two *ax/eq* conformers in the crystal structure of the same enantiomer leads to the presumption that the poor chiroptical properties could be explained based on recent conformational analyses of chiral TTF derivatives regarding the influence of the conformational changes on the intensity/pattern of the CD signals.[14] Thus, TD-DFT calculations were performed on both conformers of the *P* enantiomer, taking into account the solvent in which the experimental data were obtained (acetonitrile).

DFT investigations suggest a low energy difference between the two conformers, of ~ 0.5 kcal/mol. The calculated CD spectra of the two conformers, ***P-ax*** and ***P-eq***, together with the experimental one, are shown in ***Figure 2.4***. The two conformers present CD bands of opposite signs, suggesting a cancellation of CD signals, the result being the low CD intensity observed in the case of the experimental data.

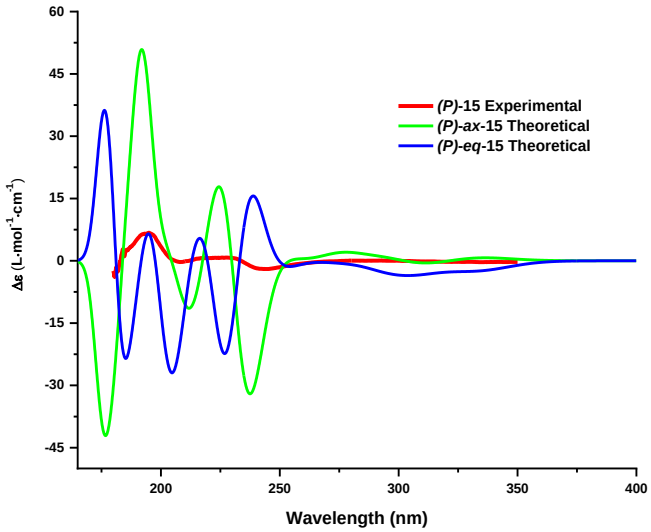


***Figure 2.4.*** CD spectra of ***(P)*-15.** Red line corresponds to the experimental data, blue and green lines to the *axial* and *equatorial* conformations

After complete structural characterization, compound ***rac*-15** was further engaged in a trimethyl phosphite mediated hetero-coupling reaction with EDT-DTT (***Scheme 2.4***). The target spiro-TTF **II** was obtained in very low yield (3-6%). All the attempts to increase the yield by varying the reaction conditions led to the obtaining of the target spiro-TTF **II** almost in traces, with many phosphonate derivatives as side products. Therefore, finding the optimal synthetic strategy that endorses the hetero-coupling reaction has not been successful so far.

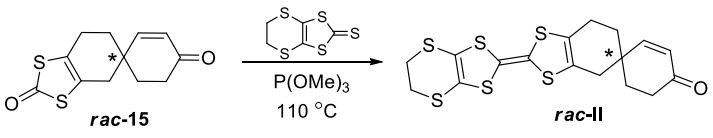


***Scheme 2.4.*** Synthesis of spiroTTF ***rac*-II**

The formation of the spiro-TTF **II** was confirmed by NMR spectroscopy, MS spectrometry and by X-Ray diffraction measurements. The chiroptical properties were investigated through ECD spectroscopy and optical rotations measurements after its chiral HPLC separation. Similar to the spiro **15**, the chiroptical activity of **II** is much lower as compared to the three chiral centre version **I**. The absolute configuration assignment to the corresponding separated enantiomer was based on the type of the Cotton effect in both target spiroTTF **II** and spiro precursor **15**.

## 2.2.3 Synthesis of radical cation salts and charge transfer complexes using spiro-TTFs

Once characterized, the target compounds **I** were used in the formation of chiral conducting materials. Thus, both racemic forms **IA** and **IB**, as well as the enantiopure ones were engaged in electrocrystallization with different anions such as $ClO_4^-$, $PF_6^-$, $AsF_6^-$, $Mo_6O_{19}^{2-}$, $I_3^-$ and in chemical oxidation with $TCNQF_4$ (2,3,5,6-Tetrafluoro-7,7,8,8-tetracyanoquinodimethane) and $TCNQF_2$ (2,5-Difluoro-7,7,8,8-tetracyanoquinodimethane). None of the attempts so far afforded suitable crystals for X-Ray diffraction measurements.

The racemic form of spiro-TTF **II**, as well as the enantiopure ones were used in the formation of molecular conducting materials by means of both electrocrystallization and chemical oxidation methods. Considering the very low yield of the hetero-coupling reaction of the synthesis of spiro-TTF **II** and the relatively big amount of donor needed for one electrocrystallization cell (~4 mg), only few attempts in obtaining charge transfer complexes were conducted, however, no radical cation salts were obtained.

For the synthesis of charge transfer complexes, $TCNQF_4$ and $TCNQF_2$ were used as chemical oxidants (1 Eq), in both dichloromethane and chloroform, for all three forms of spiro-TTF **II (*rac*, *M*** and ***P*)**. The chemical oxidation of the ***rac*-II** with $TCNQF_4$, in dichloromethane, gave a mixture of two phases (wide and narrow black plates), both of them consisting in 1:1 stoichiometry between the donor and the acceptor, while for the enantiopure forms, only one of the phases was obtained. The chemical oxidation of **II** with $TCNQF_2$ afforded suitable crystals for X-Ray diffraction measurements only in the case of the *M* enantiomer.

Resistivity measurements on **[*M*-II]TCNQF$_4$** and **[*P*-II]TCNQF$_4$** single crystals showed semiconducting behaviour of both forms with low room temperature conductivity for both enantiomers. Conductivity measurements on single crystal of the **[*rac*-II]TCNQF$_4$** and **[*M*-II]TCNQF$_2$** complexes is yet to be performed.

# Chapter 3

# Chiral fused tetrahydrofuran-TTF precursors for charge transfer complexes and radical cation salts

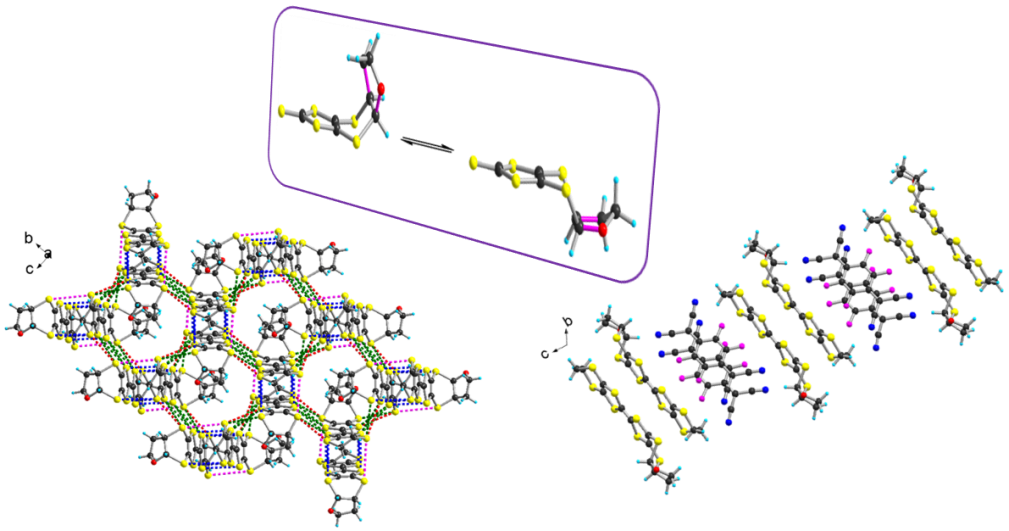

# *3.1 Literature data*

The design and synthesis of new π-donors for electroactive materials has been of great interest to chemical researchers in recent decades. Considering the large amount of conducting materials provided by the BEDT-TTF donor, the chemical modification of this backbone serves as a perfect starting point for investigating structure-properties relationships in electroactive materials.

The substitution of the ethylene bridge of EDT-DTT and BEDT-TTF by the 1,4-dioxane heterocycle, to afford donors such as bis(dioxane-dithio)-tetrathiafulvalene (BDDT-TTF), dioxane-bis(dithio)-tetrathiafulvalene (DOET), dioxane-bis(dithio)-ethylenediselena-tetrathiafulvalene (DOES) or dioxane-dithio-dihydro-tetrathiafulvalene (DODHT) (***Chart 3.1***) was reported by Kotov et al. [15] in 1994. Later, the DOET and DOES donors provided metallic radical cation salts with $Au(CN)_2^-$, $BF_4^-$ (for DOET donor) and $I_3^-$, $AuI_2^-$ (for DOES donor) anions. $(DOET)_2BF_4$ and $(DOES)_2(AuI_2)_{0.75}$ showed *β*-type crystal structures, with donor mode overlap similar to that of the *β*-$(BEDT\text{-}TTF)_2I_3$ superconductor. [16] Two superconductors based on the DODHT reduced π-system, namely ($[DODHT]_2X$, X = $PF_6^-$, $AsF_6^-$), were reported by Ishikawa et al. [17]

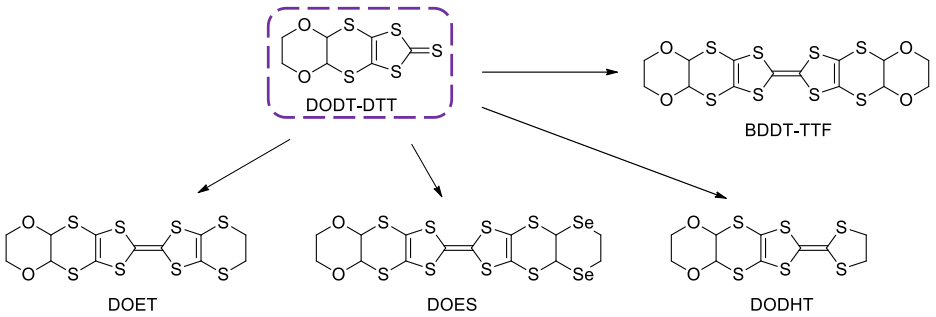


***Chart 3.1.*** TTF derivatives containing fused 1,4-dioxane heterocycles

However, all the donors depicted in ***Chart 3.1*** possess at least one mirror plane through the long axis of the molecules, and are therefore achiral. In order to induce a symmetry breaking and thus create the opportunity to access chiral donors, a non-symmetric heterocycle must be fused to the ethylenedithio-dithiolone moiety. To this purpose, we envisaged the attachment of a THF ring, instead of 1,4-dioxane, in the 2,3-positions.

## *3.2 Results*

This chapter is devoted to a novel family of chiral TTF precursors, containing a THF ring fused to the ethylenedithio fragment, and their charge transfer complexes and radical cation salts. The previously discussed 1,4-dioxane-fused EDT-TTF derivatives have proven to be important donors in the synthesis of metallic and superconducting radical cation salts, despite the steric hindrance that the 1,4-dioxane ring endows the structure with. Thus, the envisaged strategy for the access to novel series of chiral TTF derivatives implies the modification of the EDT-DTT precursor by attaching a heterocycle to it, through a stereospecific reaction (***Chart 3.2***).

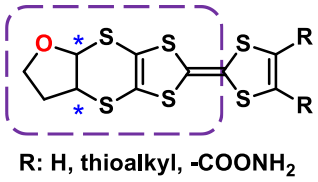


***Chart 3.2.*** General representation of the novel chiral TTF frame, bearing two stereogenic centers

### 3.2.1 Synthesis, structural, chiroptical and electronic investigation of novel chiral THF-TTFs

To gain access to new chiral TTF precursors bearing two or four stereogenic centers, the Diels-Alder reaction was accounted for the introduction of chiral centers and functionalities. Thus, 2,3-dihydrofuran (***Scheme 3.1***– left side), together with 2,5-dihydrofuran [18] (***Scheme 3.1***– right side) for comparison, were treated with trithione **T3** in refluxing toluene. Both THF-EDT-DTT **16** and **17** were obtained in a very good yield (86% and 72% respectively) and their complete structural analysis was performed. The stereospecificity of the D-A reaction, corroborated with the position of the oxygen atom relative to the double bond of the dihydrofuran ring, afforded the access to *racemic* (for compound **16**) and *meso* (for compound **17**) forms of THF-EDT-DTT (***Scheme 3.1***- bottom).

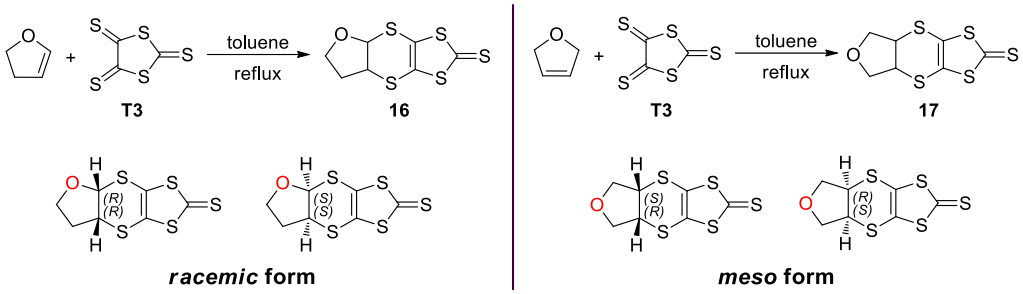


***Scheme 3.1.*** Synthesis of THF-EDT-DTT through Diels-Alder reactions (top) and configurations of the stereogenic centres of the obtained compounds (bottom)

THF-EDT-DTT **17** was further treated with $Hg(OAc)_2$ and ketone **17'** was obtained (***Scheme 3.2***). Unlike the racemic form of the THF-EDT-DTT, the *meso* form can be easily and rapidly crystallized through evaporation, using a variety of solvents. Suitable crystals for X-ray measurements were obtained for both **17** and **17'** by slow evaporation of dichloromethane solutions.

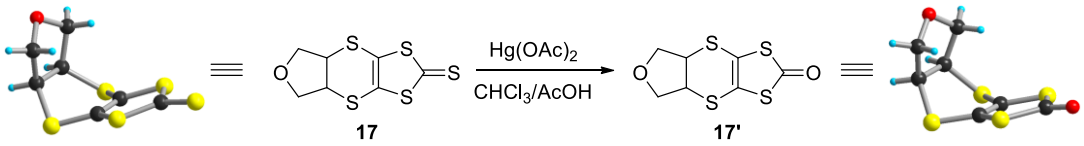


***Scheme 3.2***. Synthesis of THF-EDT-DTT **17'** (middle) and X-ray structures of **17** (left side) and **17'** (right side)

The new chiral precursor **16** was subjected to enantiomer resolution through chiral HPLC, and the chiroptical properties were investigated using ECD spectroscopy and optical rotation measurements. In order to establish the absolute configuration of the separated enantiomers and to properly analyse the spectroscopic experimental data, TD-DFT calculations were carried out.

DFT calculations were performed on the two conformers (*axial* and *equatorial*) of the (*S*,*S*)-**16**, in order to determine the equilibrium geometries and their relative energies. The solvation effects of dichloromethane have been accounted in the study. Given the resulted negligible energy gap between the two (~0.2 kcal/mol – margin of error of the method), it is safe to conclude that in solution, the two conformers can be found in similar ratio. TD-DFT calculations of the two conformers, *axial* and *equatorial*, revealed not only low intensity of the CD waves in the high wavelength range, but also CD spectra of opposite signs for the two conformers in the low wavelength range (***Figure 3.1***). Thus, the low CD intensity of compound **16** is probably due to the cancellation of the CD waves of the two conformers. Moreover, the

assignment of the (*S,S*) configuration to the first eluted enantiomer **16a** was based on the negative Cotton effect, present in both theoretical and experimental data.

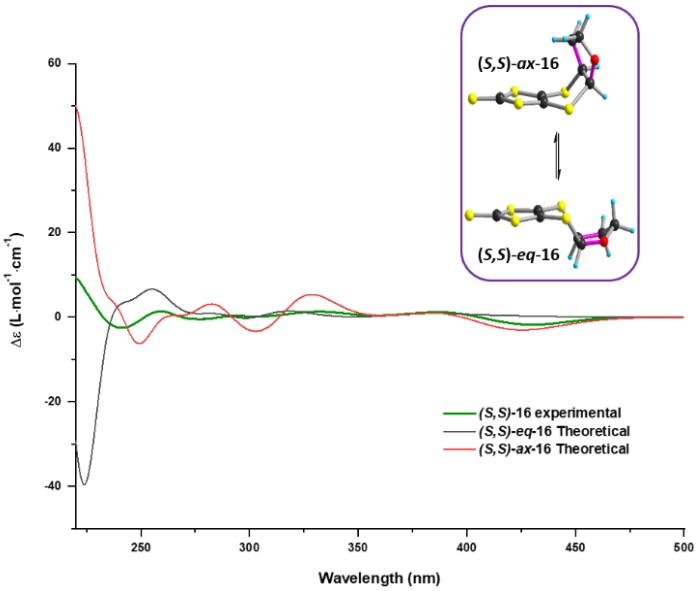


***Figure 3.1.*** Calculated and measured CD spectra of ***(S,S)*-16.** Green line corresponds to experimental data; grey and red lines correspond to theoretical data of the *axial* and *equatorial* conformers

Compound **16** was further engaged in trimethyl phosphite mediated coupling reactions with different 1,3-dithio-2-ones, in order to obtain various TTF donors based on the THF-EDT motif (***Scheme 3.3***). As illustrated below, we can easily obtain TTFs decorated with the THF motif (racemic and/or *meso*) at both ends or only at one. The aim was to get complete series of racemic, *S,S* and *R,R* forms to be further used as donors for crystalline conducting materials.

Thus, when (*rac*)**-16** has been engaged in heterocoupling reactions with ethylenedithio-dithiolone, dithiomethyl-dithiolone and di(methylcarboxylate)-dithiolone we obtained TTFs possessing stereogenic centres at one side (***Scheme 3.3***– left side) whereas, when coupled to itself or to (*meso*)**-17'** more complex structures were obtained.

For example, donor **V** (THF-BEDT-TTF-mTHF) could not be efficiently separated from the reaction mixture, due to low differences of retention factor between the obtained species. In fact, the coupling of the racemic and *meso* units gives a rather complex mixture of products. Besides the homocoupling derivatives we can form as well stereoisomers of the heterocoupling product because once attached to an asymmetric motif the *meso* form of **17'** becomes a *R,S/S,R* blocked configuration with respect to the oxygen atom contained in the chiral unit.

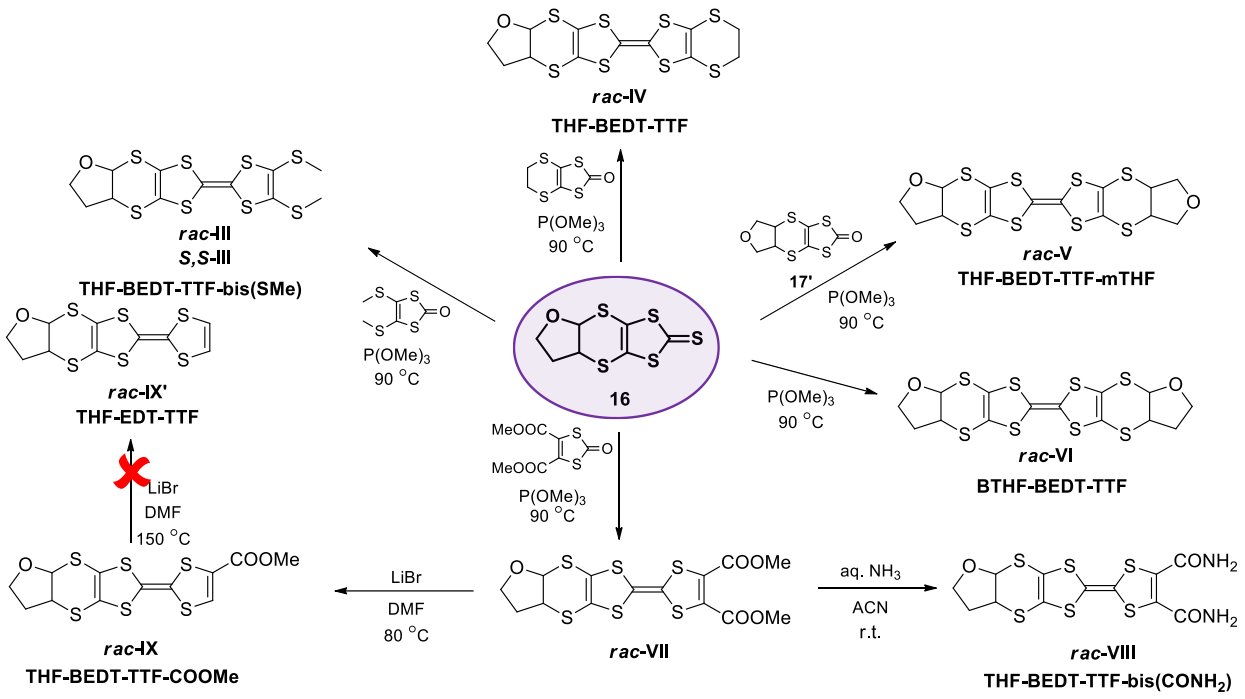


***Scheme 3.3.*** Synthesis of novel THF-EDT-DT based donors

Compounds **IV** and **VI** were separated through chiral HPLC and their chiroptical properties were investigated through ECD spectroscopy and optical rotation measurements. Also, the structures of the racemic forms of THF-TTFs **III** (THF-EDT-TTF-bis(SMe)), **IV** (THF-BEDT-TTF) and **VIII** were determined by single crystal X-ray diffraction measurements. Suitable crystals were obtained by slow evaporation of the solvent mixture for donors **III** and **IV** (v/v, dichloromethane/diethylether = 2/3 for donor **III** and dichloromethane/petroleum ether = 2/1 for donor **IV**). Single crystals of donor **VIII** were grown overnight from a concentrated DMSO solution, in air, as narrow red plates which turn dark red and became breakable when taken out of the solution.

The electronic properties of the novel TTF donors, investigated by cyclic voltammetry revealed the classical electrochemical behaviour of TTF derivatives with voltammograms showing the two reversible one-electron oxidation waves. Moreover, the additional THF unit of compound **VI** leads to a negligible impact on the electronic properties of the donor, with respect to compound **IV**. A significant difference in the oxidation potentials was observed between donors **III** and **VIII**, in which case, an anodic shift of 0.15 V and 0.13 V was observed for the latter.

## 3.2.2 Synthesis of radical cation salts and charge transfer complexes containing THF-TTF precursors

The novel THF-TTF donors were further used in the synthesis of potentially conducting molecular materials, as both charge transfer complexes (CTC) and radical cation salts (RCS).

The racemate and the *S,S* enantiomer of THF-TTF-bis(SMe) **III** were successfully used with $TCNQF_4$ as electron acceptor yielding 1:1 charge transfer complexes with low room temperature conductivity. The attempts in obtaining radical cation salts using various anions, *i.e.* $PF_6^-$, $ClO_4^-$, $ReO_4^-$, $FeBr_4^-$ and $Cu(NCS)_2^-$, were unsuccessful, probably due to the high solubility of these donors in the used solvents/solvent mixtures (***Table 3.1*** – column (1)).

A charge transfer complex of ***rac*-IV** with $TCNQF_4$ was obtained, while the enantiopure forms of donor **IV** lead every time to very small needles, therefore, no structure could be determined. Radical cation salts were successfully obtained with seven different anions ($I_3^-$, $AsF_6^-$, $Mo_6O_{19}^{2-}$, $ClO_4^-$, $ReO_4^-$, $FeBr_4^-$, $InBr_4^-$) using the racemate of donor **IV** together with the enantiopure forms for some of the anions (***Table 3.1*** – column (2)). No mixed valence salts were obtained, instead, in every case of the seven obtained radical cation salts, the donor IV monocation was present. Single crystal resistivity measurements performed on the $ClO_4^-$, $ReO_4^-$, $FeBr_4^-$, $InBr_4^-$ radical cation salts revealed semiconducting behaviour in every case.

BTHF-BEDT-TTF **VI** was engaged in the synthesis of charge transfer complexes with $TCNQF_4$ as chemical oxidant. All the four available forms of the donor (racemic, meso, *R,R,R,R* and *S,S,S,S*) have formed charge transfer complexes but the X-ray diffraction measurements were not successful because the materials were generally obtained as very small thin needles. All the attempts in synthesizing donor **VI** based radical cation salts with various anions were unsuccessful so far (***Table 3.1*** – column (3)).

The diamide **VIII** was synthesized with the aim to take advantage of the possibility to establish halogen/hydrogen bonding interactions, therefore $PF_6^-$ and $ClO_4^-$ were first used as counterions in different conditions, without any success so far. The synthesis of charge transfer complexes using the diamide **VIII** as electron-donor unit was as well unsuccessful with both $TNCQF_4$ and $TCNQF_2$ chemical oxidants, probably due to the low solubility of the donor (***Table 3.1*** – column (4)).

***Table 3.1.*** Overview on the attempted charge transfer complexes and radical cation salts syntheses

| Donor / Anion | **(1)** THF-TTF-bis(SMe) **III** | **(2)** THF-BEDT-TTF **IV** | **(3)** BTHF-BEDT-TTF **VI** | **(4)** THF-BEDT-TTF-bis($CONH_2$) **VIII** |
|---|---|---|---|---|
| $I_3^-$ | - | racemic 1:1 salt | - | - |
| $PF_6^-$ | **x** | - | - | **x** |
| $AsF_6^-$ | - | racemic 1:1 salt | **x** | - |
| $ClO_4^-$ | **x** | racemic 1:1 salt | **x** | **x** |
| $ReO_4^-$ | **x** | racemic 1:1 salt | - | - |
| $FeBr_4^-$ | **x** | racemic, (*S*,*S*), (*R*,*R*) 1:1 salt | - | - |
| $InBr_4^-$ | - | racemic 1:1 salt | - | - |
| $Cu(NCS)_2^-$ | **x** | racemic, (*R*,*R*) 1:1 salt | **x** | - |
| $Mo_6O_{19}^{2-}$ | - | racemic 2:1 salt | **x** | - |
| $TCNQF_2$ | x | too small crystals | too small crystals | **x** |
| $TNCQF_4$ | racemic, (*S*,*S*) 1:1 complex | too small crystals | too small crystals | **x** |

# Chapter 4

# Radical cation salts based on methylated EDT-TTF and BEDT-TTF

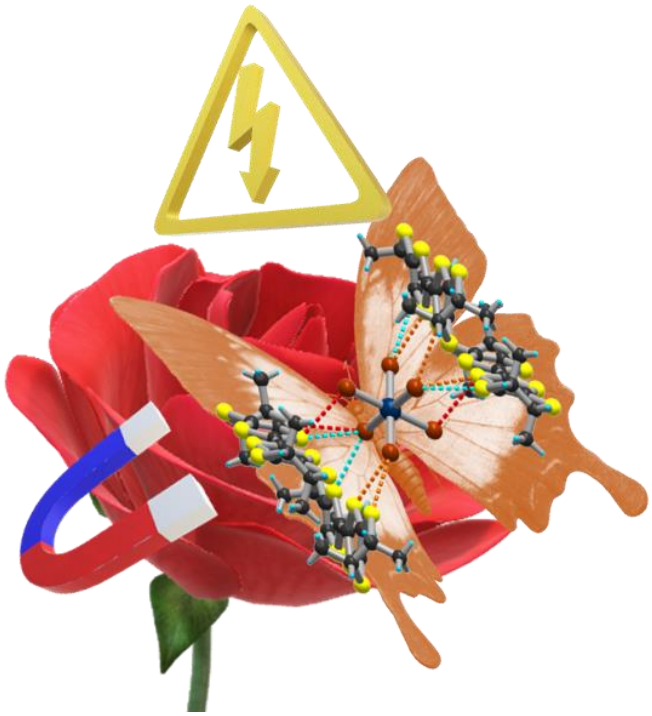

# 4.1 Introduction

The sundry amount of chiral conductive materials provided by the TTF derivatives is continuously developing, unveiling various effects and phenomena that were uncommon so far in organic materials. Among this variety of molecular materials, those provided by TM-BEDT-TTF and, more recently, by Me-EDT-TTF, represent an unwavering importance in this field. Thus, in this chapter, the focus is oriented towards the synthesis and characterization of novel molecular materials, using donors with both one (Me-EDT-TTF) and four (TM-BEDT-TTF) chiral centres (***Figure 4.1***). The two donors have been synthesized following reported procedures. [19,20]

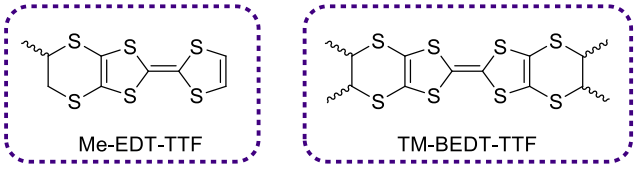


***Figure 4.1.*** Chiral donors used in the study of new chiral conducting materials

# 4.2 Results

## 4.2.1 Synthesis of radical cation salts containing chiral TTF derivatives with one and four stereogenic centres

For this study three different anions have been used in the formation of the radical cation salts (***Figure 4.2***). The synthesis was carried out using the electrocrystallization technique. $AsF_6^-$ was used as counterion with the Me-EDT-TTF donor in order to complete a previous study. [21] The $(TBA)_2IrCl_6$ and $(TBA)_2IrBr_6$ salts (TBA = tetrabutylammonium) have been provided by our collaborators at the ICMol, Valencia, Spain, and were used in electrocrystallization experiments with the TM-BEDT-TTF donor in order to obtain radical cation salts with conducting and magnetic properties.

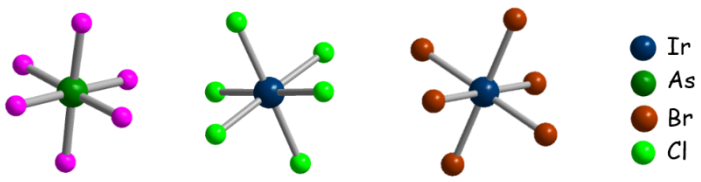


***Figure 4.2.*** General representation of the anions used in the synthesis of radical cation salts

### *4.2.1.1 Radical cation salts of TM-BEDT-TTF with Iridium anions*

Suitable crystals for X-ray measurements were obtained through electrocrystallization, by applying a constant current of 0.5 μA during seven days. The experiment in which $IrBr_6^{2-}$ was used as counterion yielded perfectly shaped black plates, whereas, when $IrCl_6^{2-}$ anion was used, dull black needles were obtained, with poor quality for X-ray diffraction (***Figure 4.3***). Surprisingly, when the experiment implying $IrBr_6^{2-}$ as counterion was carried out with the donor and the anion placed in separate compartments, two different crystals were obtained, one type corresponding to the previously obtained one, and the second one corresponding to the aspect of the crystals obtained in the case of $IrCl_6^{2-}$ radical cation salt.

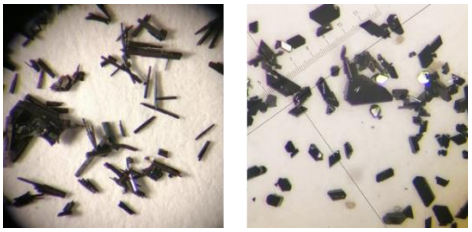

***Figure 4.3.*** Aspect of the obtained $IrCl_6^{2-}$ (left side) and $IrBr_6^{2-}$ (right side) radical cation salts

#### 4.2.1.1.1 [TM-BEDT-TTF]$_{4.5}$IrCl$_6$

**[(*4R*)-TM-BEDT-TTF]$_{4.5}$IrCl$_6$** crystallized in the non-centrosymmetric monoclinic *I*2 space group, with four independent and one half donor molecules and one independent anion in the asymmetric unit cell (***Figure 4.4***). The methyl groups are situated in the equatorial position, thus, favouring the packing of the donor molecules in the lattice. The central C=C and internal C−S bond distances suggest a mixed valence salt, however, the exact value of these bond lengths could not be determined due to the poor crystallographic data.

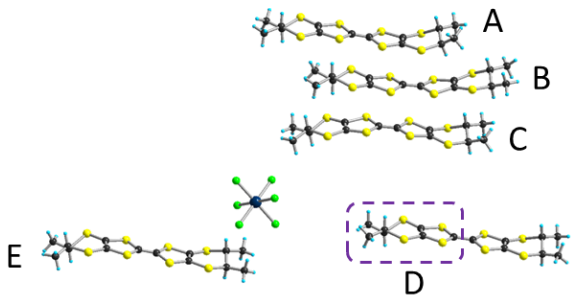


***Figure 4.4***. Molecular structure of **[(*4R*)-TM-BEDT-TTF]$_{4.5}$IrCl$_6$** radical cation salt. The half molecule of the donor, present in the asymmetric unit cell, is highlighted (left side)

Single crystal resistivity measurements of **[(*4R*)-TM-BEDT-TTF]$_{4.5}$IrCl$_6$** performed at ambient pressure show metallic behaviour between 300 – 200 K, then a transition to semiconducting behaviour is observed.

### 4.2.1.1.2 [TM-BEDT-TTF]$_2$IrBr$_6$

A complete series of isostructural (*meso*), (*rac*), (*R*,*R*,*R*,*R*) and (*S*,*S*,*S*,*S*) **[TM-BEDT-TTF]$_2$IrBr$_6$·2TCE** radical cation salts were obtained. The *racemic* and *meso* salts crystallized in the centrosymmetric triclinic *P*-1 space group, with two half donor molecules, one half anion molecule and one independent solvent molecule in the asymmetric unit cell. On the other hand, the enantiopure salts crystallized in the non-centrosymmetric triclinic *P*1 space group, with two independent donor molecules, one independent anion and two independent solvent molecules in the asymmetric unit (***Figure 4.5***). The *face-to-face* arrangement of the donor molecules is probably prevented by the methyl groups, which are located on the axial position of the EDT unit, thus providing the molecular structure with an *edge-to-edge* orientation between the donors.

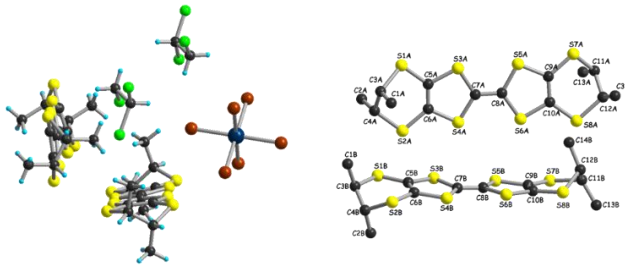

***Figure 4.5***. Asymmetric unit cell of **[(*4R*)-TM-BEDT-TTF]$_2$IrBr$_6$·2TCE** (left side) and the two independent donor molecules (right side)

Single crystal resistivity measurements were performed an all four (*meso*), (*rac*), (*R*,*R*,*R*,*R*) and (*S*,*S*,*S*,*S*) forms of **[TM-BEDT-TTF]$_2$IrBr$_6$·2TCE** radical cation salts, using the four contacts method for the enantiopure crystals, while for the *meso* and *racemic* forms, the two contacts method was used. All four salts exhibit semiconducting behaviour and have low room temperature conductivity.

Band structure calculations have been performed for the *meso* and the enantiopure forms of the **[TM-BEDT-TTF]$_2$IrBr$_6$·2TCE** radical cation salts, in order to gain insight on their electronic properties. The theoretical calculations suggest that there is a hierarchy of three types of magnetic interactions in this salt: those within the chains along *a* which are dominant, and

those along the donors inter-chain direction and the anion-donor ones which are both neatly weaker. Using appropriately larger unit cells, ground states with full AF ordering of spins can be build. However, the existence of two slightly different donor molecules, the occurrence of two relatively weak competing magnetic interactions and the structural features of the donor-anion interaction suggest that the many "local defects" occur within this fully ordered magnetic lattice. Magnetic measurements are in progress by our collaborators in Valencia.

#### 4.2.1.1.3 [TM-BEDT-TTF]$_4$IrBr$_6$

The second set of crystals, with the same aspect as in the case of the **[(*4R*)-TM-BEDT-TTF]$_{4.5}$IrCl$_6$** radical cation salt, were as well poor quality ones. This second phase crystallized in the non-centrosymmetric monoclinic *C*2 space group, with two half and three independent donor molecules and one independent anion in the asymmetric unit (***Figure 4.6***). The packing features of **[(*4R*)-TM-BEDT-TTF]$_4$IrBr$_6$** are similar to that of $IrCl_6^{2-}$ radical cation salt.

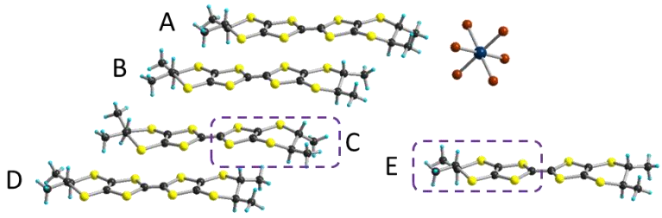


***Figure 4.6.*** Molecular structure of **[(*4R*)-TM-BEDT-TTF]$_4$IrBr$_6$**. The two independent half donor molecules present in the asymmetric unit are highlighted

### *4.2.1.2 Radical cation salts of Me-EDT-TTF with $AsF_6^-$*

Previous work done in our group regarding complete series of radical cation salts of Me-EDT-TTF included that with $AsF_6^-$ as counter anion, of 2:1 ratio between the donor and the anion. [21] The electrocrystallization experiments were carried out following the classic procedure, where the anion is present in both anodic and cathodic compartments. The **[(*rac*)-Me-EDT-TTF]$_2$AsF$_6$** salt crystallized in the centrosymmetric triclinic *P*-1 space group, with one independent donor and one half anion located on the inversion center in the asymmetric unit (***Figure 4.7*** – left side). The isostructural (*S*) and (*R*) **[Me-EDT-TTF]$_2$AsF$_6$** salts crystallized in the non-centrosymmetric triclinic *P*1 space group, with two independent donors and one independent anion in the asymmetric unit cell (***Figure 4.7***).

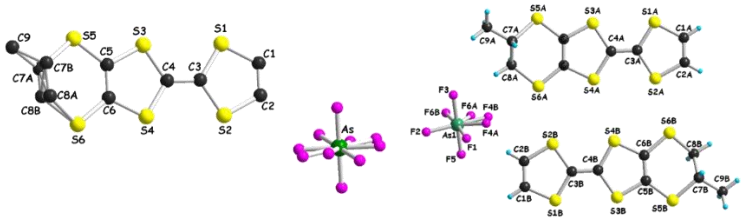

***Figure 4.7.*** Asymmetric unit cells of **[(*rac*)-Me-EDT-TTF]$_2$AsF$_6$** (left side) and **[(*S*)-Me-EDT-TTF]$_2$AsF$_6$**. H atoms on the left side have been omitted for clarity

As shown in the case of $IrBr_6^{2-}$ radical cation salts (see section ***4.2.1.1***), the presence of the anion in only one or both compartments of the electrocrystallization cell influences the ratio between the donor and the anion in the radical cation salt. In this respect, additional electrocystallization experiments have been carried out with solutions of (*S*) and (*R*)-Me-EDT-TTF donor and $AsF_6^-$ anion in THF which were placed in separate compartments. In these new conditions, black prismatic blocks of 1:1 radical cation salts were obtained. (*S*) and (*R*) **[Me-EDT-TTF]AsF$_6$·2THF** are isostructural and crystallized in the non-centrosymmetric triclinic *P*1 space group, with two independent donors, one independent anion and two independent solvent molecules in the asymmetric unit (***Figure 4.8***). The strong dimerization in the lattice, with long lateral S−S interdimer distances leads to the presumption that this salt is most probably an insulator, as opposed to the **[Me-EDT-TTF]$_2$AsF$_6$** which showed metallic behaviour in the high temperature regime.

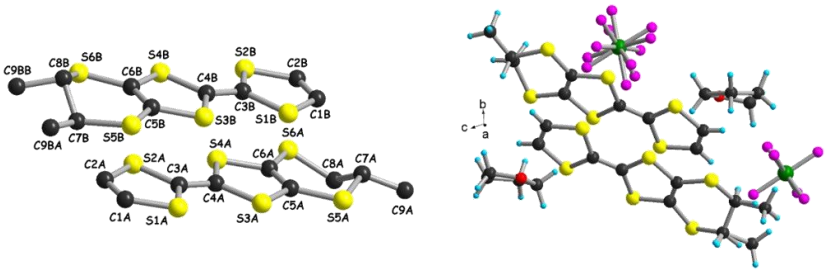

***Figure 4.8***. The two independent donor molecules in the crystal structure of **[(*S*)-Me-EDT-TTF]AsF$_6$·2THF** (left side) and the asymmetric unit cell (right side)

# Chapter 5

# Synthesis and characterization of novel miscellaneous chiral TTF derivatives

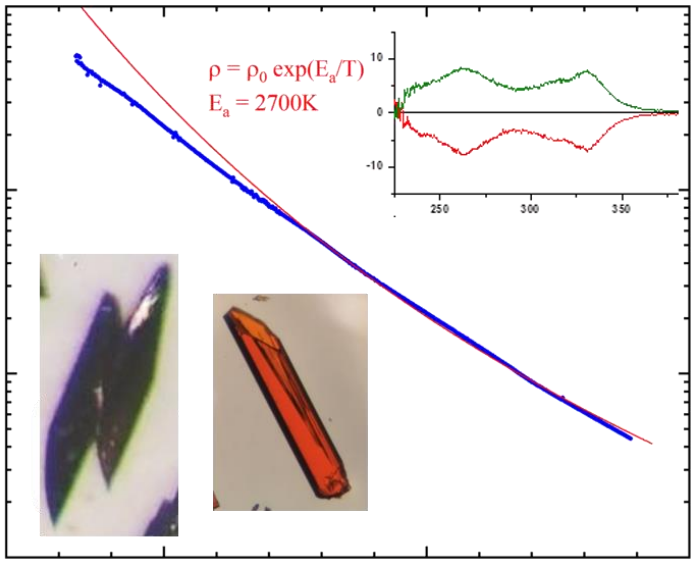

# 5.1 Introduction

This last chapter encloses the exploration of new chiral TTFs in the context of novel conductive molecular materials. To this effect, several chiral precursors, presented in ***Chart 5.1***, were considered for the synthesis of the targeted TTF based donors.

Spiro racemic compounds **9A** and **9B**, previously synthesized and characterized in *Chapter 2*, are resumed for the association with the (*meso*)-THF-EDT-DTT unit **17'**.

The DM-EDT-DTT precursor **18**, previously used in the group, was further employed in the synthesis of new chiral donors, bearing two different functionalities on the opposite side of the TTF framework.

Finally, compound **19** was used in the synthesis of chiral diamides, bearing two TTF units.

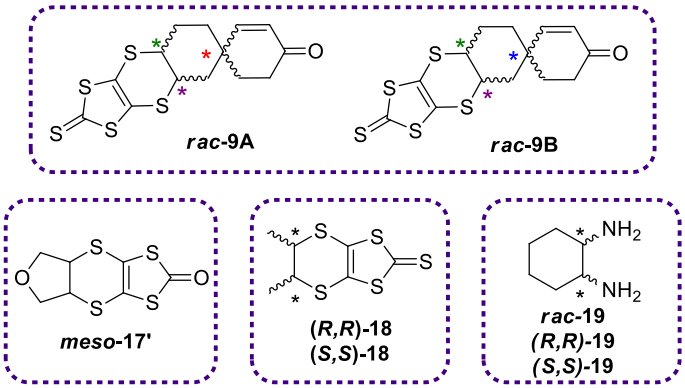


***Chart 5.1.*** Precursors employed in the synthesis of novel TTF based donors

# 5.2 Results

## 5.2.1 Spiro-THF-TTF systems

The gathered knowledge provided by both spiro-TTFs and THF-TTFs chapters influenced the design of new spiro-THF-TTF systems. Thus, spiro racemics **9A** and **9B** have been engaged in a trimethyl phosphite mediated heterocoupling reaction with (*meso*)-THF-EDT-DTT **17'** (***Scheme 5.1***). The target compounds ***rac*-XIA** and ***rac*-XIB** were obtained in very low yields, 8% and 6% respectively, due to the previously discussed combined effects of the retro-Diels-Alder reaction and Arbuzov rearrangements.

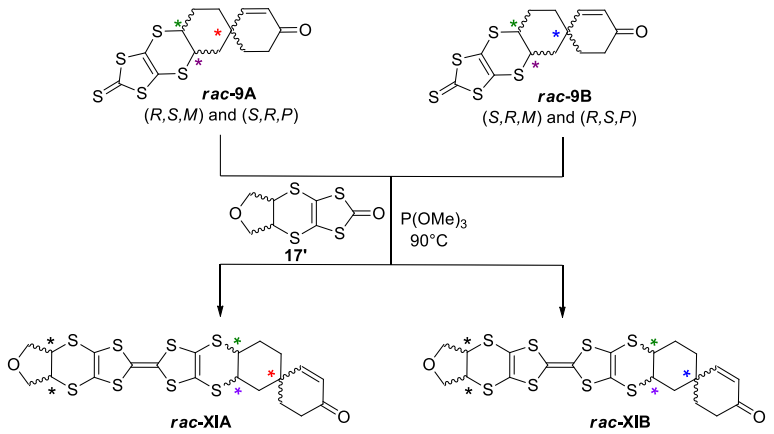


***Scheme 5.1***. Synthesis of spiro-THF-TTF systems ***rac*-XIA** and ***rac*-XIB**

Similar to the case of compound **V**, here as well, when attached to the spiro motif, the *meso* form of the THF-EDT unit becomes a blocked *R/S* and *S/R* configuration. Thus, the product of each of the two coupling reactions consists actually in a mixture of diastereomers (***Figure 5.1***). Although the resulting systems contain five chiral centres each, the $2^n$ (where n = number of the stereogenic centres) rule is not fulfilled, due to the nature of the starting substrates. Therefore, for each enantiomer of the two racemic forms of compound **9**, there are two possibilities for the fixation of the *meso* compound **17'**, either *R/S* or *S/R*, resulting a mixture of two pairs of enantiomers per racemic form.

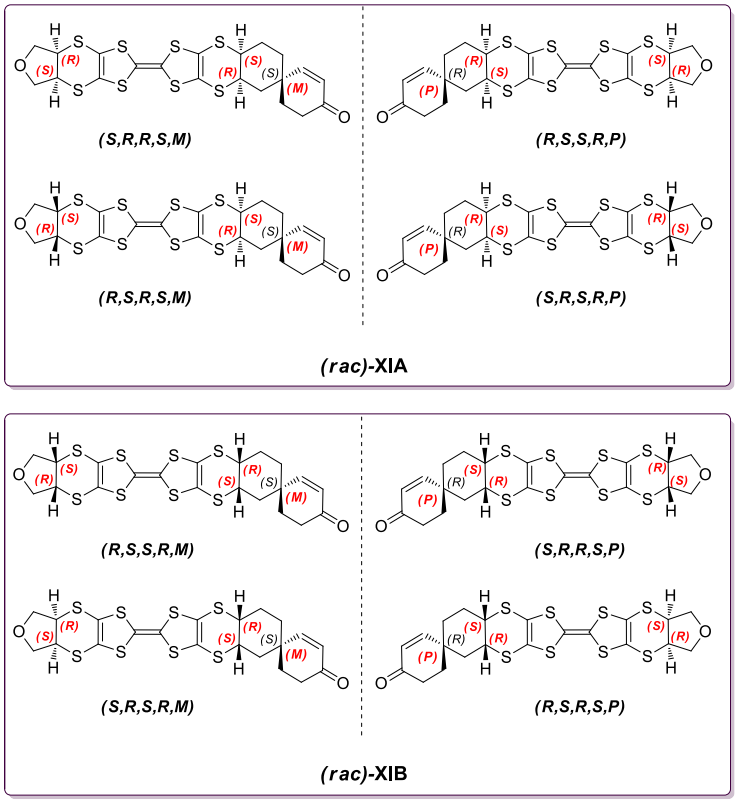


***Figure 5.1.*** Representation of ***rac*-XIA** (top) and ***rac*-XIB** (bottom) isomers

The attempts to crystallize the racemates of the neutral donors **XI** by several crystallization techniques led to only small needles that were not suitable for single crystal X-ray measurements. The chemical oxidation experiments, using TCNQ, $TCNQF_2$ or $TCNQF_4$ as oxidants, led to very small needles of charge transfer complexes, thus, no structural data of these species were obtained. Electrocrystallization experiments were carried out using $ClO_4^-$ and $PF_6^-$ as counterions, in different conditions, yet, no radical cation salts were obtained so far. All these unsuccessful attempts are very likely due to the mixtures of isomers of ***rac*-XIA** and ***rac*-XIB**. Their chiral HPLC is yet to be performed.

## *5.2.2 Donors based on DM-EDT-DTT*

During the last decade, the DM-EDT-DTT **18** chiral precursor provided important series of TTF based conductive molecular materials. The possibility of having interesting packing patterns in the lattice, by introducing a THF unit or an amide group in the DM-EDT-TTF framework, led to the design and synthesis of novel the TTF derivatives **XII** and **XIII**.

The enantiopure forms of **18** were engaged in a phosphite mediated heterocoupling reaction with ***meso*-17'** compound, and **(*R,R*)** and **(*S,S*)-XII** donors were obtained in 17% (*R,R*) and 26% (*S,S*) yields (***Scheme 5.2***). The formation of the target compounds was confirmed by NMR spectroscopy and MS spectrometry. The chiroptical and electronic properties of compounds XII were investigated as well, using ECD spectroscopy and cyclic voltammetry.

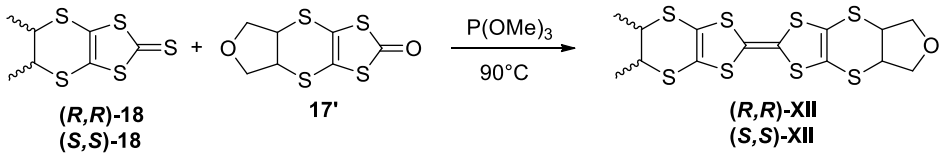


***Scheme 5.2.*** Synthesis of ***(R,R)*** and **(*S,S*)-XII**

So far, the different crystallization techniques tested on the neutral donors **(*R,R*)-XII** and **(*S,S*)-XII** provided only very small needles, which could not be measured. Several attempts in synthesizing charge transfer complexes and radical cation salts using these enantiopure donors were unsuccessful, yet work on finding the right conditions is in progress.

The enantiopure compounds **18** were engaged in a phosphite mediated heterocoupling reaction with the diester derivative as well, in order to obtain compounds **20**. Following the multi-step synthetic strategy presented in ***Scheme 5.3*** the target compound **XIII** was obtained ai a fine precipitate. The obtained precipitate could not be investigated through NMR spectroscopy, nor through CD, UV-Vis or cyclic voltammetry due to the low solubility. The formation of the desired compound was confirmed thanks to MS analysis, together with that of the bis(TTF) product **XIII'**. The structure of **(*S,S*)-XIII** was confirmed as well by X-ray diffraction measurements performed on long orange needles grown in DMSO during four days.

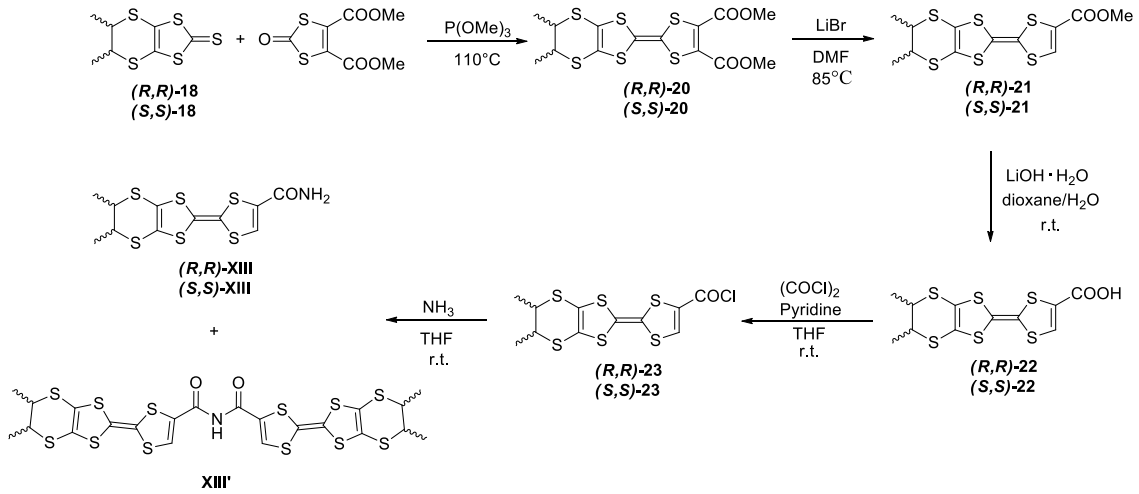


***Scheme 5.3***. Synthesis of **(*R,R*)-XIII** and **(*S,S*)-XIII** monoamides

Despite their low solubility, compounds **XIII** are promising candidates for the synthesis of electroactive materials, if the right conditions for the synthesis of such materials are found. [22,23, 24]

## *5.2.3 1,2-diaminocyclohexane based diamide donors*

The racemic, *R,R* and *S,S* forms of compound **XIV** were obtained following the same multi-step synthetic strategy as for the synthesis of the enantiopure compounds **XIII**. Thus, acyl chloride **27**, obtained in a four steps strategy, was engaged without purification in a substitution reaction with 1,2-cyclohexanediamide **19** (*racemic*, *R,R* and *S,S*), in THF, in the presence of $Et_3N$ (***Scheme 5.4***). The target diamides **XIV** were obtained in good yields (54%, 74%, 66%) after chromatographic separation, and the formation of the desired compounds were confirmed by NMR spectroscopy and MS spectrometry.

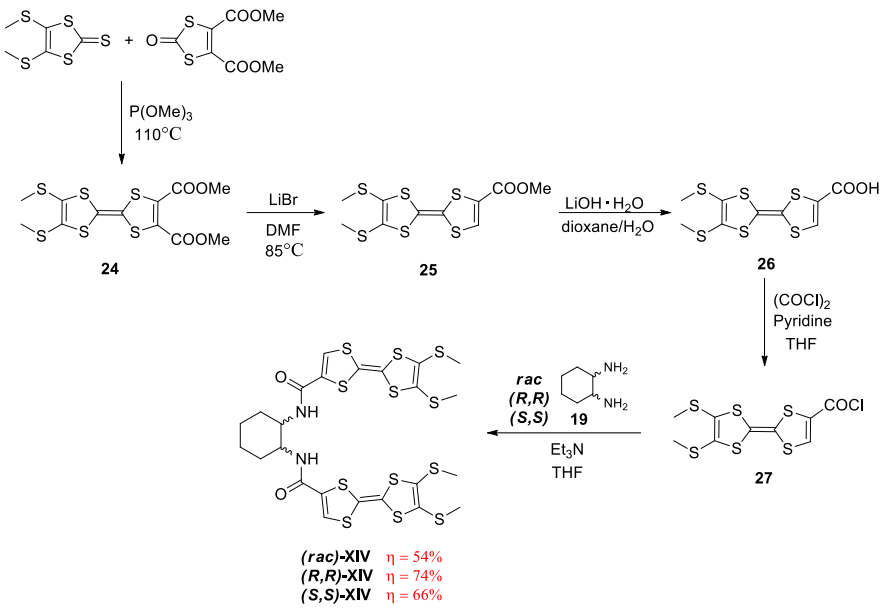


***Scheme 5.4***. Synthesis of diamides **XIV**

In order to investigate the absorption behaviour of the oxidized **(*rac*)-XIV** compound, its oxidation was performed chemically, using $FeCl_3$ as oxidant, in DCM solution, at room temperature, and monitored through UV-Vis measurements (***Figure 5.2***). The emergence of the two bands at 552 and 762 nm typical for $TTF^{+\bullet}$, along with the decrease in intensity of the 325 nm band, suggest the formation of the radical cation. After the addition of 4 equivalents of $FeCl_3$, the oxidation process is complete. The oxidized species seem quite stable, as suggested by the absorption spectra of the oxidized solution measured after one week (green line).

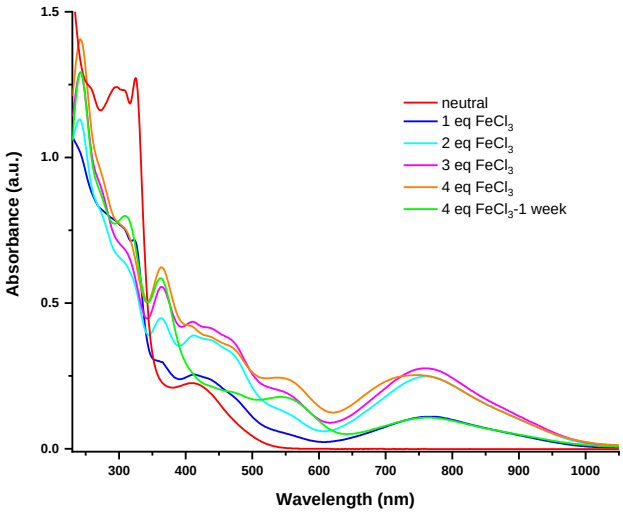


***Figure 5.2.*** UV-Vis absorption spectra of **(*rac*)-XIV** during chemical oxidation by successive addition of $FeCl_3$ in DCM, at room temperature

While for the racemic form of compound **XIV** suitable crystals for X-ray measurements were obtained, in the case of the enantiopure compounds, although interesting hollow tube-shaped crystals were obtained, no structure could be determined (***Figure 5.3*** – left side). Narrow plaquettes like, orange crystals of ***(rac)*-XIV** were obtained by slow evaporation of the solvent mixture (v/v, DCM/EE = 3/2). ***(rac)*-XIV** crystallized in the centrosymmetric triclinic *P*-1 space group, with two independent molecules, A and B, in the asymmetric unit.

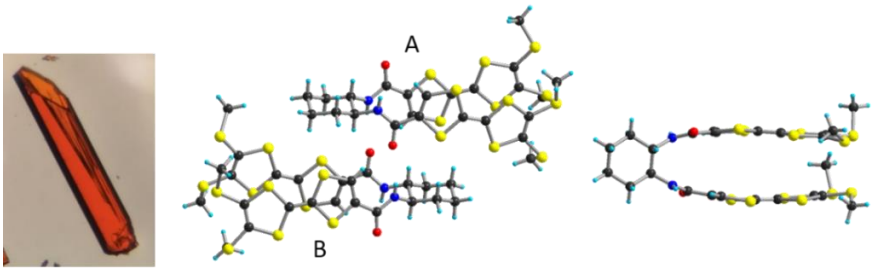


***Figure 5.3.*** Aspect of the obtained crystals of enantiopure **XIV** (left side) and the asymmetric unit structure of **(*rac*)-XIV** (right side)

The three **XIV** donors (*racemic*, *R*,*R* and *S*,*S*) were engaged in electrocrystallization experiments, carried out with several anions, *i.e.* $PF_6^-$, $AsF_6^-$, $ClO_4^-$, $ReO_4^-$, $I_3^-$. In the case of the enantiopure compounds no crystals were obtained out of the electrocrystallization cells, yet, the racemic form provided several radical cation salts. Although robust and well-defined crystals were obtained, no structure of these radical cation salts could be determined, due to the low quality of the crystals.

Resistivity measurements on single crystals of the radical cation salt of **(*rac*)-XIV** and $AsF_6^-$ were performed. The temperature dependence of the electrical resistivity indicates a semiconducting behaviour of this radical cation salt, with a room temperature conductivity of $1.6 \cdot 10^{-6}$ $S \cdot cm^{-1}$, and an activation energy of 2700 K.

# General conclusions of the PhD thesis

This thesis enhances the chiral TTF derivatives family through novel TTF systems where axial and point chirality are present.

New spiro-TTF precursors and donors have been synthesized and their chiroptical activity was investigated. Significant difference of behaviour was observed between the diastereomers of the spiro precursors and TTFs with three chiral centres, the most remarkable being a difference of ~ 200 degrees in optical rotations. Considerably lower chiroptical properties were determined in the case of the new compounds with one chiral centre, as compared to the three chiral centres ones. However, the poor results obtained in the chiroptical investigations was later explained by the presence of two conformational isomers in solution, having opposite signs in CD.

New category of chiral TTF donors has been developed, that are the THF fused chiral TTFs. THF-EDT-TTF-bis(SMe) and THF-BEDT-TTF provided charge transfer complexes with $TCNQF_4$ acceptor, that showed low room temperature conductivity. Structural features of seven radical cations salts of THF-BEDT-TTF with different anions have been discussed and single crystal resistivity measurements performed on the $ClO_4^-$, $ReO_4^-$, $FeBr_4^-$ and $InBr_4^-$ radical cation salts showed semiconducting behaviour in every case.

Novel radical cation salts of TM-BEDT-TTF and Me-EDT-TTF have been prepared. It was shown that the method used for the preparation of the electrocrystallization cell influences the ratio between the donor and acceptor in the final material. The radical cation salt of TM-BEDT-TTF with $IrBr_6^{2-}$ magnetic anion shows semiconducting properties and has a metamagnetic behaviour at 17 K and a slow relaxation of the magnetization below this temperature.

Finally, four other chiral TTFs have been synthesized, namely spiro-BEDT-TTF-THF, DM-BEDT-TTF-THF, DM-EDT-TTF-$CONH_2$ and cyclohexane-diamide-bis(TTF). Except the monoamide DM-EDT-TTF-$CONH_2$, the structure and properties investigations of the newly synthesized molecules were carried out. The X-ray diffraction structures of amides DM-EDT-TTF-$CONH_2$ and cyclohexane-diamide-bis(TTF) are also reported.

# Perspectives of the Phd thesis

On the basis of the results obtained during this thesis, the perspectives cover different directions, as follows:

**1)** Finding suitable conditions of electrocrystallization for the spiro-TTF donors is needed, in order to have access to complete series of radical cation salts. The synthesis of extended spiro-TTFs is also envisaged either through functionalization of the available carbonyl group of spiro core **8**, or by the activation of the double bond vicinal to the carbonyl group through catalysed Diels-Alder reaction. In this respect, Wittig-Horner reaction on the spiro core 8 and on the spiro-EDT-DTT 9 have already been carried out (***Figure P.4***). Considering the obtained low yield of this type of reaction, the best strategy seems to be the functionalization of the carbonyl group after the spiro-TTFs I and II are formed.

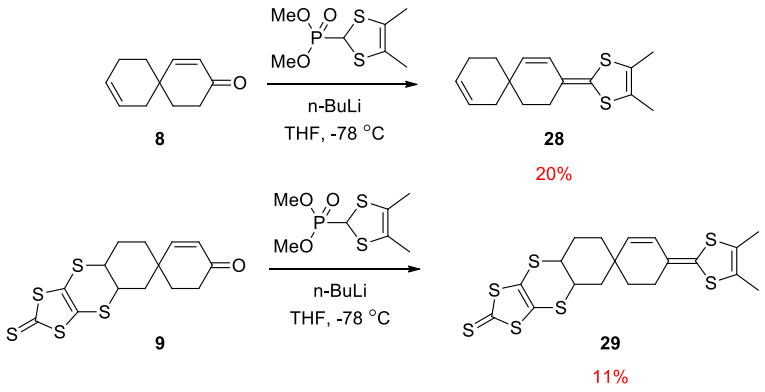


***Figure P.4.*** Wittig-Horner reactions on spiro derivatives 8 and 9

**2)** Preparation of complete series of radical cation salts of the THF-TTF donors, since for now, only THF-BEDT-TTF based radical cation salts have been obtained. Also, the synthesis of THF-EDT-TTF and THF-EDT-TTF-monoamides are envisaged (***Figure P.5***).

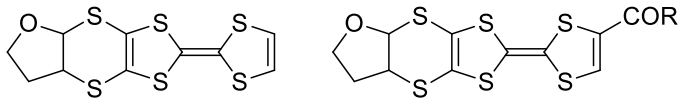


***Figure P.5.*** Envisaged THF-EDT-TTF and THF-EDT-TTF-monoamides

**3)** After obtaining the TM-BEDT-TTF magnetic conductors with iridium based anions, other representative chiral TTFs, such as DM-BEDT-TTF or DM-EDT-TTF, will be engaged in the synthesis of radical cation salts with iridium magnetic anions.

**4)** Since the last chapter mainly consists in the synthesis, structural, chiroptical and electronic investigations of the new TTF derivatives, future work will be dedicated to the preparation of radical cation salts of these chiral donors with various anions.

**5)** Based on the experience of our group in chiral metal-bis(dithiolene) complexes [25,26], the novel chiral precursors represent suitable ligands for this kind of materials. First attempts of complexation reactions of spiro-EDT-DTT 9 to Ni(II) metal were unsuccessful, hence, the ketone form of spiro precursor **9** was synthesized (***Figure P.6*** – top). Moreover, Ni(II)-bis(dithiolene) complex using the THF-EDT-DTT precursor has been synthesized (***Figure P.6*** – bottom) and its formation was confirmed by MS analysis, however, no crystals were obtained so far. Further work on metal-bis(dithiolene) complexes synthesis with the THF-EDT-DTT, but also with the spiro chiral precursors is currently carried out in the group. Transition metal ions, such as Ni(II), Au(III), Pd(II) and/or Pt(II) will be used for this study.

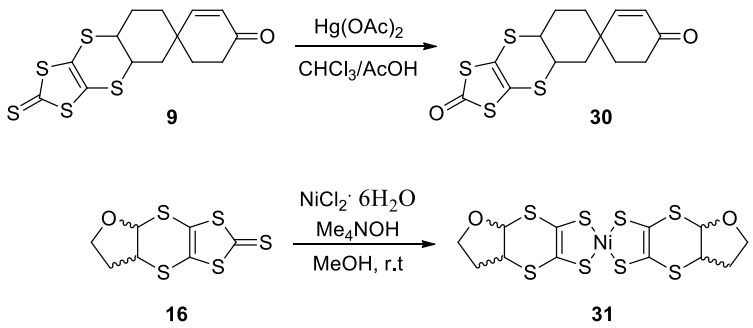


***Figure P.6***. Trans-chalcogenation reaction of compound 9 (top) and the synthesis of the Ni(II)-bis(dithiolene) complex with THF-EDT-DTT 16 (bottom)

**6)** Considering the experience of our group in Cluj in organic solar cells, [27,28,29] the obtained chiral TTF will be investigated as donors in single material organic solar cells (SMOSCs). The influence of chirality on the solar cells properties have not yet been studied. In this respect, donor **32** and the fullerene based SMOSC **33** have been synthesized and the structure-properties relationship has been investigated, [30] in order to be further used as a reference for the chiral TTF based solar cells (***Figure P.7***).

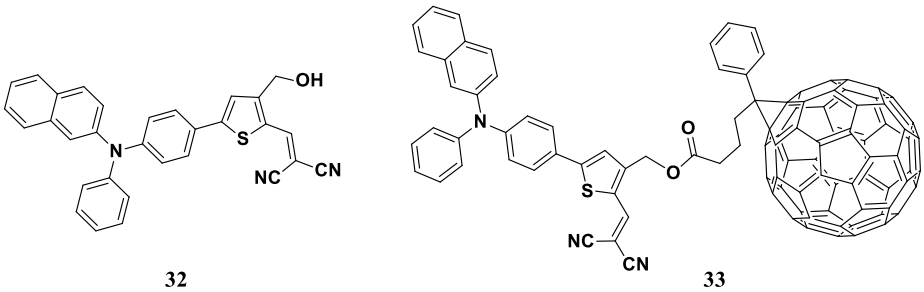


***Figure P.7.*** Arylamine based donor and single material organic solar cell

# References


[1] a) J. L. Segura, N. Martin, *Angew. Chem. Int. Ed.* 2001, *40*, 1372–1409; b) D. Canevet, M. Sallé, G. X. Zhang, D. Q. Zhang, D. B. Zhu, *Chem. Commun.* 2009, 2245–2269.

[2] (a) J. M. Williams, J. R. Ferraro, R. J. Thorn, K. D. Carlson, U. Geiser, H. H. Wang, A. M. Kini, M.-H. Whangbo *Organic Superconductors (Including Fullerenes), Synthesis, Structure, Properties and Theory* (Grimes, R. N. ed., Prentice-Hall, Englewoods Cliffs, NJ, 1992); (b) special issue *Chem. Rev.* 2004, *104*, no 11 "*Molecular Conductors*", ed. P. Batail

[3] N. Avarvari, J. D. Wallis, *J. Mater. Chem.* 2009, *19*, 4061–4076.

[4] a) C. Réthoré, N. Avarvari, E. Canadell, P. Auban-Senzier, M. Fourmigué, *J. Am. Chem. Soc.* 2005, *127*, 5748–5749; b) A. M. Madalan, C. Réthoré, M. Fourmigué, E. Canadell, E. B. Lopes, M. Almeida, P. Auban-Senzier, N. Avarvari, *Chem. Eur. J.* 2010, *16*, 528–537.

[5] a) F. Pop, P. Auban-Senzier, A. Frąckowiak, K. Ptaszyński, I. Olejniczak, J. D. Wallis, E. Canadell, N. Avarvari, *J. Am. Chem. Soc.* 2013, *135*, 17176–17186; b) F. Pop, P. Auban-Senzier, E. Canadell, N. Avarvari, *Chem. Commun.* 2016, *52*, 12438–12441.

[6] F. Pop, P. Auban-Senzier, E. Canadell, G. L. J. A. Rikken, N. Avarvari, *Nature Commun.*, 2014, 5:3757, doi: 10.1038/ncomms4757.

[7] T. Biet, A. Fihey, T. Cauchy, N. Vanthuyne, C. Roussel, J. Crassous, N. Avarvari, *Chem. Eur. J.* **2013**, 19, 13160–13167.

[8] Y. Zhou, D. Zhang, L. Zhu, Z. Shuai, D. J. Zhu, *Org. Chem.* 2006, *71*, 2123−2130.

[9] M. Hasegawa, Y. Sone, S. Ywata, H. Matsuzawa, Y. Mazaki, *Org. Lett.*, **2011**, *13*, 4688-4691.

[10] a) E. Nishikawa, H. Tatemitsu, Y. Sakata, S. Misumi *Chem. Lett.* 1986, 2131-2134; b) H. Tatemitsu, E. Nishikawa, Y. Sakata, S. Misumi *Synth. Met.* 1987, *19*, 565-568.

[11] P. Sadin, A. Martinez-Grau, L. Sanchez, C. Seoane, R. Pou-Amerigo, E. Orti, N. Martin, *Org. Lett.* 2005, *7(2)*, 295-298.

[12] M. Hasegawa, D. Kurebayashi, H. Matsuzawa, Y. Mazaki *Chem. Lett.* 2018, *47(8)*, 989-992.

[13] J.-P. Griffiths, H. Nie, R. J. Brown, P. Day, J. D. Wallis, *Org. Biomol. Chem.*, **2005**, *3*, 2155-2166.

[14] A. Abhervé, N. Mroweh, T. Cauchy, F. Pop, H.-B. Cui, R. Kato, N. Vanthuyne, P. Alemany, E. Canadell, N. Avarvari, *J. Mater. Chem. C*, 2021, *9*, 4119–4140.

[15] A. I. Kotov, K. Faulmann, P. Cassoux, E. B. Yagubskii, *J. Org. Chem*. **1994**, *59*, 2626-2629.

[16] a) J. Yamada, S. Tanaka, H. Anzai, T. Sato, H. Nishikawa, I. Ikemoto, K. Kikuchi, *J. Mater. Chem*., **1997**, *7*, 1311-1312. b) H. Nishikawa, H. Ishikawa, T. Sato, T. Kodama, I. Ikemoto, K. Kikuchi, S. Tanaka, H. Anzai, J. Yamada, *J. Mater. Chem* **1998**, *8*, 1321-1322. c) J. Yamada, H. Nishikawa, K. Kikuchi, *J. Mater. Chem* **1999**, *9*, 617-628.

[17] H. Ishikawa, T. Morimoto, T. Kodama, I. Ikemoto, K. Kikuchi, J. Yamada, H. Yoshino, K. Murata, *J. Am. Chem. Soc.* **2002**, 124(5), 730-731.

[18] Y. Yamashita, M. Tomura, K. Imaeda, *Mol. Cryst. Liq. Cryst.* **2002,** *380***,** 203-207.

[19] N. Mroweh, P. Auban-Senzier, N. Vanthuyne, E. Canadell, N. Avarvari, *J. Mater. Chem. C* 2019, *7*, 12664–12673.

[20] a) J. D. Wallis, A. Karrer, J. D. Dunitz, *Helv. Chim. Acta.*, 1986, *69*, 69-70; b) F. Pop, P. Auban-Senzier, A. Frackowiak, K. Ptazynsky, I. Olejniczak, J. D. Wallis, E. Canadell, N. Avarvari, *J. Am. Chem. Soc.*, 2013, *135*, 17176-17186.

**[21]** N. Mroweh, A. Bogdan, F. Pop, P. Auban-Senzier, N. Vanthuyne, E. B. Lopes, M. Almeida, N. Avarvari, *Magnetochemistry* 2021, *7*, 87.

**[22]** A. Saad. O. Jeannin, M. Fourmigue, *CrystEngComm*, 2010,***12***, 3866-3874.

**[23]** S. A. Baudron, N. Avarvari, P. Batail, C. Coulon, R. Clerac, E. Canadell, P. Auban-Senzier, *J. Am. Chem. Soc.* 2003, *125*, 38, 11583–11590.

**[24]** N. Mroweh, F. Pop, C. Meziere, M. Allain, P. Auban-Senzier, N. Vanthuyne, P. Alemany, E. Canadell, N. Avarvari, *Cryst. Growth Des.* 2020, *20*, 4, 2516–2526.

**[25]** D. G. Branzea, F. Pop, P. Auban-Senzier, R. Clerac, P. Alemany, E. Canadell, N. Avarvari, *J. Am. Chem. Soc*, 2016, *138*, 6838-6851.

**[26]** A. Abherve, N. Mroweh, T. Cauchy, F. Pop, H. Cui, R. Kato, N. Vanthuyne, P. Alemany, E. Canadell, N. Avarvari, *J. Mater. Chem. C*, 2021, *9*, 4119-4140.

**[27]** N. Terenti, G.-I. Giurgi, A.-P. Crisan, C. Anghel, A. Bogdan, A. Pop, I. Stroia, A. Terec, L. Szolga, I. Grosu, J. Roncali *J. Mater. Chem. C*, **2022,***10*, 5716-5726**.**

**[28]** A. P. Diac, L. Szolga, C. Cabanetos, A. Bogdan, A. Terec, I. Grosu, J. Roncali, *Dyes and Pigments*,

**2019**, *171*, 107748; DOI: 10.1016/j.dyepig.2019.107748.

**[29]** J. Roncali, I. Grosu, *Adv.Sci*. 2019, *6*, 1801026.

**[30]** A. Bogdan, L. Szolga, G.-I. Giurgi, A. P. Crișan, D. Bogdan, S. Hadsadee, S. Jungsuttiwong, R. Po, I. Grosu, J. Roncali, *Dyes and Pigments* **2021**, *184*, 108845.

Titlu: Derivați chirali de tetratiafulvalenă ca precursori pentru conductori moleculari cristalini

**Cuvinte cheie:** tetratiafulvalenă, chiralitate, spiro-TTF, structuri cristaline, Diels-Alder, conductivitate, magnetism, electrocristalizare

**Rezumat:** Sinteza și utilizarea tetratiafulvalenelor chirale ca precursori pentru conductori moleculari chirali s-au dezvoltat continuu în ultimul deceniu, determinate de mai multe observații cu privire la multifuncționalitatea acestora. În urma asocierii chiralității cu electroactivitatea diverse particularități ale materialelor obținute au fost observate, cum ar fi conductivitate diferită între formele racemice și enantiopure, modularea redox a proprietăților chiroptice sau detectarea efectului de anizotropie magnetochirală în conductorii enantiopuri cristalini în *bulk*.

În acest studiu, interesul este orientat înspre sinteza, investigarea structurală, chiroptică și electronică a noi precursori chirali de TTF pentru materiale conductoare, precum și înspre utilizarea acestor derivați în materiale electroactive.

Prima parte a proiectului este dedicată atât sintezei și caracterizării unor derivați spiranici de TTF cu unul și cu trei centri chirali, cât și caracterizării complecșilor cu transfer de sarcină bazate pe spiro-TTFi cu un centru chiral.

A doua parte a proiectului constă în sinteza și caracterizarea a noi derivați de TTF cu unități THF condensate, cu doi sau patru centri chirali, precum și în utilizarea acestora în materiale conductoare chirale.

A treia parte descrie noi materiale conductoare bazate pe Me-EDT-TTF și TM-BEDT-TTF cu anioni magnetici și non-magnetici.

În final, sinteza și caracterizarea unor diverși noi derivați de TTF chirali sunt discutate în ultima parte, contribuind astfel la provocarea obținerii de noi materiale electroactive.

Title: Chiral tetrathiafulvalene precursors for crystalline molecular conductors

**Keywords:** tetrathiafulvalene, chirality, spiro-TTF, crystalline structures, Diels-Alder, conductivity, magnetism, electrocrystallization

**Abstract:** The synthesis and use of chiral TTFs as precursors for chiral molecular conductors have been continuously developing over the last decade driven by several observations regarding their multi-functionality. The association of chirality with electroactivity led to various particularities of the obtained materials, such as different conductivity between the racemic and enantiopure forms, redox modulation of the chiroptical properties or the detection of magnetochiral anisotropy effect in bulk crystalline enantiopure conductors.

In this study, the focus is oriented towards synthesis, structural, chiroptical and electronic investigation of new TTF precursors for conducting materials, bearing axial and point chirality, as well as towards the use of these derivatives in electroactive materials.

The first part of the study is focused on the synthesis and characterization of spiro-TTFs with one and three chiral centres, and the characterization of charge transfer complexes based on spiro-TTF with one chiral centre.

The second part includes the synthesis and characterization of tetrahydrofuran fused TTF derivatives with two and four stereogenic centers, together with their use in chiral conducting materials.

The third part describes series of novel conducting materials based on Me-EDT-TTF and TM-BEDT-TTF donors with magnetic and non-magnetic anions.

Finally, the synthesis and characterization of new miscellaneous chiral TTF donors are discussed in the last part, thereby, contributing to the challenge in the synthesis of new electroactive materials with interesting packing and conducting properties.